Biochimica et Biophysica Acta 1847 (2015) 514–525

Contents lists available at ScienceDirect

Biochimica et Biophysica Acta

journal homepage: www.elsevier.com/locate/bbabio

Increased reactive oxygen species production during reductive stress: The roles of mitochondrial glutathione and thioredoxin reductases

Paavo Korge [a,b], Guillaume Calmettes [a,b], James N. Weiss [a,b,c,*]

[a] UCLA Cardiovascular Research Laboratory, David Geffen School of Medicine at UCLA, Los Angeles, CA 90095, United States
[b] Department of Medicine (Cardiology), David Geffen School of Medicine at UCLA, Los Angeles, CA 90095, United States
[c] Department of Physiology, David Geffen School of Medicine at UCLA, Los Angeles, CA 90095, United States

ARTICLE INFO

Article history:
Received 12 September 2014
Received in revised form 9 February 2015
Accepted 12 February 2015
Available online 19 February 2015

Keywords:
Mitochondria
ROS production
Reductive stress

ABSTRACT

Both extremes of redox balance are known to cause cardiac injury, with mounting evidence revealing that the injury induced by both oxidative and reductive stress is oxidative in nature. During reductive stress, when electron acceptors are expected to be mostly reduced, some redox proteins can donate electrons to O_2 instead, which increases reactive oxygen species (ROS) production. However, the high level of reducing equivalents also concomitantly enhances ROS scavenging systems involving redox couples such as NADPH/$NADP^+$ and GSH/GSSG. Here our objective was to explore how reductive stress paradoxically increases net mitochondrial ROS production despite the concomitant enhancement of ROS scavenging systems. Using recombinant enzymes and isolated permeabilized cardiac mitochondria, we show that two normally antioxidant matrix NADPH reductases, glutathione reductase and thioredoxin reductase, generate H_2O_2 by leaking electrons from their reduced flavoprotein to O_2 when electron flow is impaired by inhibitors or because of limited availability of their natural electron acceptors, GSSG and oxidized thioredoxin. The spillover of H_2O_2 under these conditions depends on H_2O_2 reduction by peroxiredoxin activity, which may regulate redox signaling in response to endogenous or exogenous factors. These findings may explain how ROS production during reductive stress overwhelms ROS scavenging capability, generating the net mitochondrial ROS spillover causing oxidative injury. These enzymes could potentially be targeted to increase cancer cell death or modulate H_2O_2-induced redox signaling to protect the heart against ischemia/reperfusion damage.

1. Introduction

Both the production and removal of reactive oxygen species (ROS) in the mitochondrial matrix play critical roles regulating mitochondrial function. ROS-induced redox modifications of mitochondrial proteins are required for redox signaling to adjust metabolism to changing conditions and to regulate cell death and survival pathways. Conventionally, an excess of ROS and reactive nitrogen species (RNS) relative to reducing equivalents is defined as oxidative stress. Conversely, a relative shortage of ROS compared with reducing equivalents in the form of redox couples (GSH/GSSG, NADPH/$NADP^+$, NADH/NAD^+, etc.) is defined as reductive stress [1]. However, the latter definition is somewhat confusing because in isolated mitochondria, reductive stress, in the form of high matrix NADH/NAD^+ ratios, is known to promote excessive ROS production to a level exceeding ROS scavenging capability, resulting in net H_2O_2 spillover from mitochondria [2]. Specifically, experiments have demonstrated that ROS production by alamethicin-permeabilized mitochondria increases steeply at high NADH/NAD ratios [3], which is traditionally attributed to complex I of the respiratory chain, but can also involve certain tricarboxylic acid cycle (TCA) enzymes, specifically those containing lipoamide dehydrogenase, the ROS-producing E3 component of alpha-ketoglutarate dehydrogenase and pyruvate dehydrogenase [3].

When the NADH/NAD^+ pool becomes highly reduced, so does the NADPH/$NADP^+$ pool, which increases matrix antioxidant power to compensate for increase in ROS production and limit ROS spillover. NADPH is a key reducing equivalent supplying the major H_2O_2 scavenging systems in the matrix, the glutathione/glutathione peroxidase3 (Gpx)/glutathione reductase (GR) and the peroxiredoxin3 (Prx)/thioredoxin2 (Trx)/thioreductase2 (TrxR2) systems (Fig. 1). Although catalase is also present in the matrix [4,5], it has a much lower affinity for H_2O_2 [6] and therefore is not likely to play an important role at micromolar concentrations of H_2O_2. Thus, matrix antioxidant power is ultimately dependent on

Abbreviations: CDNB, 1-chloro-2,4-dinitrobenzene; FCCP, trifluorocarbonylcyanide phenylhydrazone; GDH, glutamate dehydrogenase; GR, glutathione reductase; Gpx1, glutathione perioxidase; GSH, reduced glutathione; GSSG, oxidized glutathione; H_2O_2, hydrogen peroxide; ICDH, isocitrate dehydrogenase; pCMB, p-chloromercuribenzoic acid; pCMPS, p-chloromercuriphenyl-sulphonate; Prx, peroxiredoxin; $O_2^{\cdot-}$, superoxide; TCA, tricarboxylic acid; TrxR1, thioredoxin reductase 1; TrxR2, thioredoxin reductase 2; Trx, thioredoxin 1 and 2

* Corresponding author at: Department of Medicine (Cardiology), School of Medicine, University of California Los Angeles, Los Angeles, CA 90095, United States. Tel.: +1 310 825 9029; fax: +1 310 206 5777.
E-mail address: jweiss@mednet.ucla.edu (J.N. Weiss).

http://dx.doi.org/10.1016/j.bbabio.2015.02.012
0005-2728/

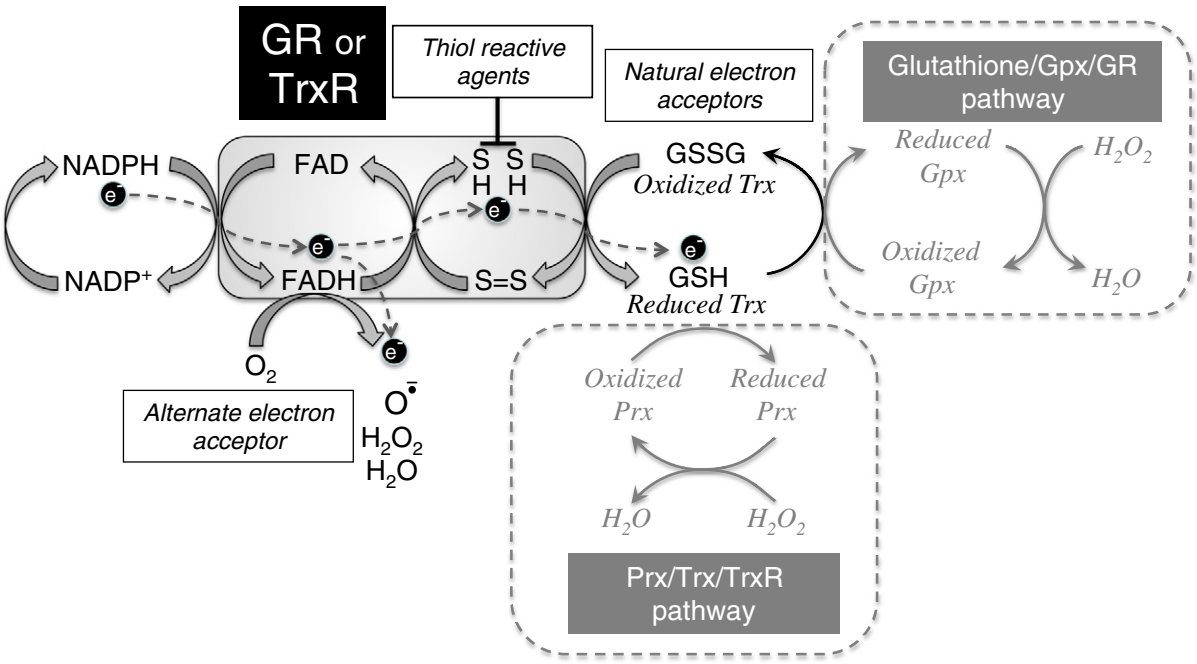

Fig. 1. Proposed mechanism of ROS generation by GR and TrxR2 during reductive stress. Flow of electrons (e^-) as indicated from NADPH to FAD to cysteine-related sulfhydryl groups (S) and then to the natural electron acceptors GSSG for GR, and oxidized Trx for TrxR2. If oxidized GSSG or Trx is in limited supply, the flavin reduction state is increased and electron flow is shunted from $FADH_2$ to O_2 as an alternative electron acceptor, with one-electron reduction producing superoxide, two-electron reduction producing H_2O_2 or four-electron reduction producing H_2O. Similarly, thiol reactive agents which react with SH groups in GR or TrxR2 also prevent electron transfer to the natural electron acceptors, resulting in superoxide, H_2O_2 and H_2O production instead.

an adequate supply of NADPH generated by transhydrogenase, isocitrate dehydrogenase, malic enzyme and glutamate dehydrogenase to keep the matrix NADPH/$NADP^+$ pool reduced.

However, experimental evidence indicates that the enhancement of antioxidant power by the reduced NADPH/$NADP^+$ pool during reductive stress is insufficient to counterbalance the increased ROS production resulting from the reduced NADH/NAD^+ pool, leading to net ROS spillover, matrix oxidation, cytotoxicity and protein aggregation causing cardiomyopathy [7–10]. These observations and others support the "redox-optimized ROS balance" hypothesis recently put forth by O'Rourke and colleagues [11,12]. According to this hypothesis, redox balance is lost and ROS production increases at both extremes of oxidation and reduction of redox couples involved in respiratory chain activity (NADH/NAD^+) or ROS scavenging (NADPH/$NADP^+$, GSH/GSSG). In other words, the extent of ROS production is defined by the overall change of matrix redox environment in either direction. In a highly reduced environment, ROS production is accelerated to the point that it overwhelms ROS scavenging capacity, even though the latter should be maximally potentiated [11,12].

To better understand the factors that lead to net ROS production and oxidative cytotoxicity during reductive stress, we explored the possibility that two of the NADPH-dependent reductases that normally enhance antioxidant function, namely GR and TrxR2, begin to directly generate significant ROS when the NADPH/$NADP^+$ pool becomes highly reduced. This hypothesis is based on the premise that these enzymes belong to the same family of disulfide reductase flavoenzymes as lipoamide dehydrogenase, the E3 component of α-ketoglutarate dehydrogenase and pyruvate dehydrogenase. Lipoamide dehydrogenase has been shown to produce ROS with a rate equal to or even higher than complex I when the NADH/NAD^+ pool is highly reduced [3,13]. It is structurally similar and catalyzes the transfer of electrons between pyridine nucleotides and disulfides with very similar reaction chemistry as GR and TrxR's. Indeed, the cytoplasmic isoform of thioredoxin reductase (TrxR1) has been previously shown to generate ROS robustly in the presence of NADPH when its preferred endogenous substrate, oxidized thioredoxin 1 (Trx), is in limited supply [14]. Under these conditions, it is thought that the reduced flavoprotein redox site of TrxR1 directly donates electrons obtained from NADPH to molecular O_2, to generate superoxide and H_2O_2 by one or two electron reduction of O_2, respectively.

In this study, we tested the hypothesis that, analogous to lipoamide dehydrogenase and TrxR1, GR and TrxR2 generate ROS when their natural electron acceptors (GSSG and oxidized Trx, respectively) are in limited supply, as illustrated schematically in Fig. 1. Using recombinant GR and TrxR1, we show that both enzymes generate robust amounts of H_2O_2 when provided with NADPH in the absence of their preferred electron acceptors, or in the presence of inhibitors which interfere with electron transfer to their preferred electron acceptors (Fig. 1). Moreover, we present evidence that these same reactions occur with GR and TrxR2 in cardiac mitochondria exposed to reductive stress, and that the amounts of ROS generated under these conditions are quantitatively comparable to those generated by respiratory complexes and TCA cycle dehydrogenases during reductive stress. Finally, we show that ROS spillover during reductive stress is very sensitive to Prx inhibition by Zn^{2+}. These findings help to explain how respiratory complexes and NAD^+-related matrix dehydrogenases, together with GR and TrxR2 directly generating ROS, combine to overwhelm NADPH-dependent antioxidant mechanisms, resulting in ROS efflux from the matrix during reductive stress.

2. Material and methods

This study was approved by the UCLA Chancellor's Animal Research Committee (ARC 2003-063-23B) and performed in accordance with the Guide for the Care and Use of Laboratory Animals published by the United States National Institutes of Health (NIH Publication No. 85-23, revised 1996) and with UCLA Policy 990 on the Use of Laboratory Animal Subjects in Research (revised 2010).

All measurements were carried out using customized Fiber Optic Spectrofluorometer (Ocean Optics) in a continuously stirred cuvette at room temperature (22 to 24 °C). The cuvette was partially open to air during isolated mitochondria experiments, but was tightly closed when O_2 consumption by recombinant GR was measured. Mitochondria

were isolated from rabbit and mouse hearts as described previously [15]. Recombinant proteins (5–400 nM) were added to incubation buffer containing 110 mM KCl, 10 mM Hepes, pH 7.4 with Tris. Mitochondria (0.5 to 1.0 mg/ml) were permeabilized with addition of alamethicin (20 μg/ml) to sucrose buffer (250 mM sucrose, 10 mM HEPES, pH 7.4 with Tris). Alamethicin creates pores which allow equilibration of low-molecular weight components across the inner membrane, while high-molecular weight proteins are retained in the matrix and intermembrane space [16]. Rat recombinant TrxR1 and Trx from *Escherichia coli* (oxidized form) were obtained from Cayman Chemical. Nox2 inhibitor gr91ds-tat was from Eurogentec. Other reagents, including recombinant human GR, recombinant human Prx 1, oxidized glutathione (GSSG), 1-chloro-2,4-dinitrobenzene (CDNB), p-chloromercuribenzoic acid (pCMB), auranofin, mersalyl, p-chloromercuriphenyl-sulphonate (pCMPS), trifluorocarbonylcyanide phenylhydrazone (FCCP), rotenone and antimycin, were obtained from Sigma. For experiments with isocitrate dehydrogenase, we used commercially available enzymes purified by Sigma.

Mitochondrial O_2 consumption was measured continuously by monitoring buffer O_2 content using a fiber optic oxygen sensor FOXY-AL300 (Ocean Optics) [17].

H_2O_2 release from mitochondria or production by recombinant GR or TrxR was measured using 10 μM Amplex UltraRed and 0.2 U Horse Radish Peroxidase (HRP) in the buffer (excitation/emission, 540/590 nm).

NAPDH oxidation by GR or TrxR1 was measured by the rate of decrease in fluorescence (366/460 nm, excitation/emission) after adding NADPH (50 μM) to the cuvette.

2.1. Statistical analysis

For each data set, the median and 95% confidence intervals (CI) are reported. The conventional percentile bootstrap-resampling approach with 10,000 replications was used for estimating 95% confidence intervals (CI) as well as examining the significant difference between groups (effect size statistics) [18–20]. A P value <0.05 was considered statistically significant.

3. Results

3.1. NADPH-dependent ROS production by purified recombinant GR

To determine whether GR is capable of generating ROS when provided with NADPH in the absence of its natural electron acceptor, as hypothesized in Fig. 1, we added purified recombinant GR at different concentrations (50 to 400 nM) to KCl buffer in the absence of GSSG (Fig. 2A). Addition of 100 μM NADPH to GR rapidly initiated H_2O_2 production that was dependent on the GR concentration. Subsequent addition of catalase (2 μM) rapidly inhibited further H_2O_2 increase. NADPH addition in the absence of GR increased fluorescence very slowly, which rapidly increased after GR addition (Fig. 2A, lower red trace). Inset shows the dependency of H_2O_2 production (in nmoles/min) on GR concentration ($n = 2$). In contrast, when GSSG was provided as the natural electron acceptor for GR, NAPDH addition did not stimulate significant H_2O_2 production (Fig. 2B, blue trace b versus red trace a). The GSSG concentration required for 50% inhibition of NADPH-induced production of ROS by GR (IC50) was 106 μM when fit to a Hill equation (Fig. 2C).

Organic mercurial compounds such as pCMB have a high affinity for thiols and at least one functionally important thiol in GR is known to react with soluble thiol reactive agents *in vitro* [21]. Binding of thiol reactive agents to reduced SH-groups interferes with electron flow from reduced pyridine nucleotides via FAD and thiol groups to GSSG (Fig. 1). Consistent with this mechanism, pCMB (50 μM) accelerated NADPH-induced H_2O_2 production by GR by 3.2-fold (95% CI [3.1, 3.3], $n = 3$), even when GSSG was present (2.2-fold increase, 95% CI [2.1, 2.4], $n = 4$) (Fig. 2B, green and purple traces *c* and *d*, respectively). Like pCMB, other organic mercurial thiol reactive agents such as mersalyl and pCMPS also increased NADPH-dependent H_2O_2 production (Fig. 2D) (2.7-fold increase, 95% CI [2.5, 2.8], and 8.3-fold increase, 95% CI [7.9, 8.6], for mersalyl ($n = 4$) and pCMPS ($n = 4$), respectively).

Fig. 2E shows NADPH consumption by GR under the same conditions as in Fig. 2B. With no GSSG present, the rate of NADPH consumption increased in parallel as the rate of H_2O_2 production was accelerated by adding mersalyl (blue trace *b*) or pCMPS (green trace *c*). Note that in the absence of mersalyl or pCMPS, addition of GR's natural electron acceptor GSSG abruptly increased NADPH consumption by many orders of magnitude (red trace *a*), indicating that the rate of electron transfer to GSSG is extremely fast compared to its maximal rate of electron leak to O_2 when no GSSG is present. In the presence of mersalyl (blue trace *b*) or pCMPS (green trace *c*), GSSG had no effect on the rate of NADPH consumption, as expected if electron transport from NADPH to GSSG is blocked. However, addition of the reducing agent DTT (1 mM) rapidly reversed the effects of mersalyl and pCMPS, causing NADPH consumption to accelerate rapidly, again by orders of magnitude. Further additions of NADPH were also rapidly consumed.

In Fig. 3, we quantitatively analyzed the relationship between NADPH consumption, O_2 consumption and H_2O_2 production rates by GR, which averaged 76.9, 42.7 and 6.5 nmol/min/mg enzyme respectively in the presence of 5 μM mersalyl (Fig. 3A), and 269.1, 143.0 and 18.8 nmol/min/mg enzyme respectively in the presence of 5 μM pCMPS (Fig. 3B). In both cases, the rates of NADPH and O_2 consumption are much greater than can be accounted for by H_2O_2 production via two-electron reduction of O_2. Specifically, assuming that one NADPH and one O_2 molecule are consumed for each H_2O_2 molecule produced, the amounts of NADPH and O_2 consumption unaccounted for by H_2O_2 production are $(76.9–6.5) = 70.4$ and $(42.7–6.5) = 36.2$ nmol/min/mg enzyme with mersalyl present, and 250.3 and 124.2 nmol/min/mg enzyme with pCMPS present. The ratio of the NADPH oxidized to O_2 consumed that is not accounted for by H_2O_2 production is thus similar and near 2.0 in both cases (1.94 for mersalyl and 2.02 for pCMPS). To demonstrate that the NADPH consumption under these conditions was directly linked to O_2 consumption, we performed the same experiment in the absence of O_2 (Fig. 3B, *inset*). Under anaerobic conditions, pCMPS did not induce NADPH oxidation by GR, and NADPH fluorescence only decreased after O_2 was readmitted. Besides two-electron reduction of O_2 to generate H_2O_2, other possible reactions that could consume NADPH include one-electron reduction of O_2 to form $O_2^{\bullet-}$, four-electron reduction of O_2 to form H_2O [22] or uptake of electrons by the added mercurial compounds. The first possibility was excluded by including superoxide dismutase (15 U/ml) in the cuvette, which did not enhance NADPH-induced H_2O_2 production by GR (data not shown). In principle, the second possibility could account for all of the remaining NADPH consumption, assuming that two NADPH molecules are reduced for each O_2 molecule to generate two H_2O molecules, assuming that GR is capable of this reaction. However, we cannot exclude that the third possibility is also important. Despite this limitation, the findings collectively indicate that ROS production by reduced GR depends on the rate of electron transport from NADPH to GSSG: leak of electrons to O_2 to form H_2O_2 is insignificant when GSSG reduction is fast, but becomes appreciable when oxidized substrate is absent or electron transport is inhibited at the level of functionally important thiols by pCMB, mersalyl or pCMPS.

3.2. NADPH-dependent ROS production by purified recombinant TrxR1

Since recombinant TrxR2 with intact enzymatic activity was not commercially available, we used recombinant TrxR1 (the cytoplasmic isoform) as a proxy, under the assumption that the matrix isoform TrxR2 is likely to have similar properties. Fig. 4A demonstrates that recombinant TrxR1 generates H_2O_2 in the presence of NADPH when its natural electron acceptor, oxidized Trx, is absent. When 100 μM NADPH was added to recombinant TrxR1 in KCl buffer, H_2O_2 generation increased rapidly in proportion to the added TrxR1 concentration. The

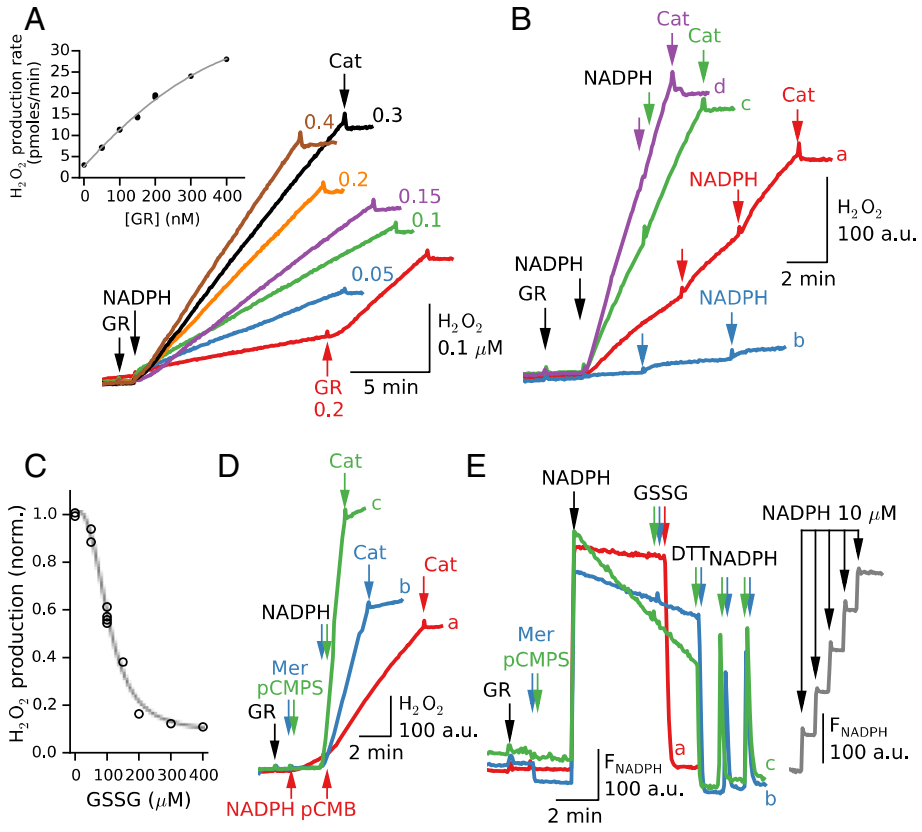

Fig. 2. NADPH-induced H_2O_2 production by recombinant GR. A. Recombinant GR was added to KCl buffer in the concentrations indicated on the traces (0.05 to 0.4 μM). Addition of NADPH (100 μM) initiated an increase in H_2O_2 production detected by resorufin fluorescence that was dependent on [GR]. In the absence of GR, NADPH had little effect on resorufin fluorescence until GR addition was also added (red trace). Inset shows the H_2O_2 production (in pmol/min) as a function of GR concentration ($n = 2$). B. Recombinant GR (200 nM) was added to KCl buffer in the absence of GSSG. Addition of 25 μM NADPH rapidly initiated H_2O_2 production (red trace *a*). Subsequent additions of 50 and 100 μM NADPH caused slight further increases in H_2O_2 production. When the same experiment was performed with 1 mM GSSG present to provide GR with its natural electron acceptor (see Fig. 1), no significant H_2O_2 production was induced by NADPH (blue trace *b*). The thiol reactive agent pCMB (50 μM) markedly accelerated NADPH-induced H_2O_2 production by GR, both in the presence (green trace *c*) and absence (purple trace *d*) of GSSG. C. GSSG-induced inhibition of H_2O_2 production by GR (100 nM) incubated with 25 μM NADPH. H_2O_2 production rates were fitted to a Hill equation with half-maximal inhibition occurring at 106 μM. D. Similar protocol showing that in the absence of GSSG, addition of 50 μM NADPH initiated H_2O_2 production by GR that was further accelerated by 5 μM pCMB (red trace *a*). At the same concentration (5 μM), other thiol reactive agents mersalyl (blue trace *b*) and pCMPS (green trace *c*) were even more potent at stimulating NADPH-dependent H_2O_2 production by GR. Note, that these chemicals had no effect on H_2O_2 production when added before NADPH. E. Corresponding traces of NADPH consumption by GR in the absence (red trace *a*) and presence of 5 μM mersalyl (blue trace *b*) or pCMPS (green trace *c*). Note that addition of 0.5 mM GSSG rapidly accelerated NADPH consumption in the absence of mersalyl or pCMPS, but had no effect in their presence until 1 mM DTT was added to reverse their inhibition of GR. (Additions to both traces are indicated by black arrows; additions to one trace only are indicated by the same color arrows).

control case with no TrxR1 (red trace labeled "0") showed only a very small nonspecific increase in resorufin fluorescence upon NADPH addition. The inset to Fig. 4A summarizes H_2O_2 production in nmoles/min for different TrxR1 concentrations. When expressed per mg protein, H_2O_2 production rate by TrxR1 averaged 8.3 nmoles/mg/min (95% CI [7.9, 8.8], $n = 8$), about 8 times higher than H_2O_2 production by GR (1.02 nmoles/mg/min, 95% CI [1.0, 1.1], $n = 7$) in the absence of inhibitors.

Fig. 4B shows that the rate of NADPH-induced H_2O_2 production by TrxR1 (50 nM) saturated between 10 and 25 μM NADPH. The TrxR1 inhibitor CDNB (50 μM) increased H_2O_2 production at each NADPH concentration. For 50 μM NADPH, the increase was 3-fold, from 8.3 nmol/mg/min to 25.1 nmol/mg/min (95% CI [21.9, 27.9], $n = 6$), as shown in Fig. 4C, which compares the average values of NADPH-dependent H_2O_2 production by TrxR1 and GR in the absence and presence of inhibitors, respectively.

We also examined the effects of oxidized Trx on NADH oxidation and H_2O_2 production by recombinant TrxR1 (Fig. 4D and E). NADPH is consumed by TrxR to reduce oxidized Trx, which is thought to be available at low micromolar levels in the matrix [23]. In the absence of both TrxR1 and Trx, NADPH fluorescence was stable in KCl buffer (Fig. 4D, red trace). Subsequent addition of TrxR1 caused NADPH oxidation at a low rate, which was further accelerated by 3.4-fold (95% CI [3.2, 3.5], $n = 3$) upon addition of CDNB (50 μM). Under the same conditions, the blue trace shows that addition of oxidized Trx (10 μM) transiently stimulated rapid NADPH oxidation by TrxR1 until all of the Trx was reduced, which was repeated again with 2.5 μM oxidized Trx. Fig. 4E shows the corresponding rates of H_2O_2 production. The oxidized Trx decreased NADPH-induced H_2O_2 production by TrxR1 in a concentration-dependent manner, with 10 μM oxidized Trx causing a 2.4-fold decrease (95% CI [2.2, 2.6], $n = 3$) that was relieved by CDNB (red trace).

Matrix NADPH concentration is expected to be in large excess relative to Trx. In addition, reduced Trx reacts with H_2O_2 rather slowly (rate constant 1.05 M^{-1} s^{-1}) [24]. Therefore, H_2O_2 detoxification in the matrix depends on reduced Prx, whose cysteine residues react directly and rapidly with H_2O_2 (rate constant 10^7 M^{-1} s^{-1} [24]). Once oxidized, Prx becomes inactive and requires donation of electrons from reduced Trx to scavenge H_2O_2 again. This is illustrated with purified TrxR1 in Fig. 5A. When TrxR1 was added to KCl buffer containing NADPH (green trace), H_2O_2 production was initiated. Addition of 1 μM oxidized Trx had no immediate effect on H_2O_2 production, but addition of Prx (100 nM) rapidly inhibited further increases in resorufin fluorescence, which remained stable even after CDNB (50 μM) was added. If CDNB was added first to

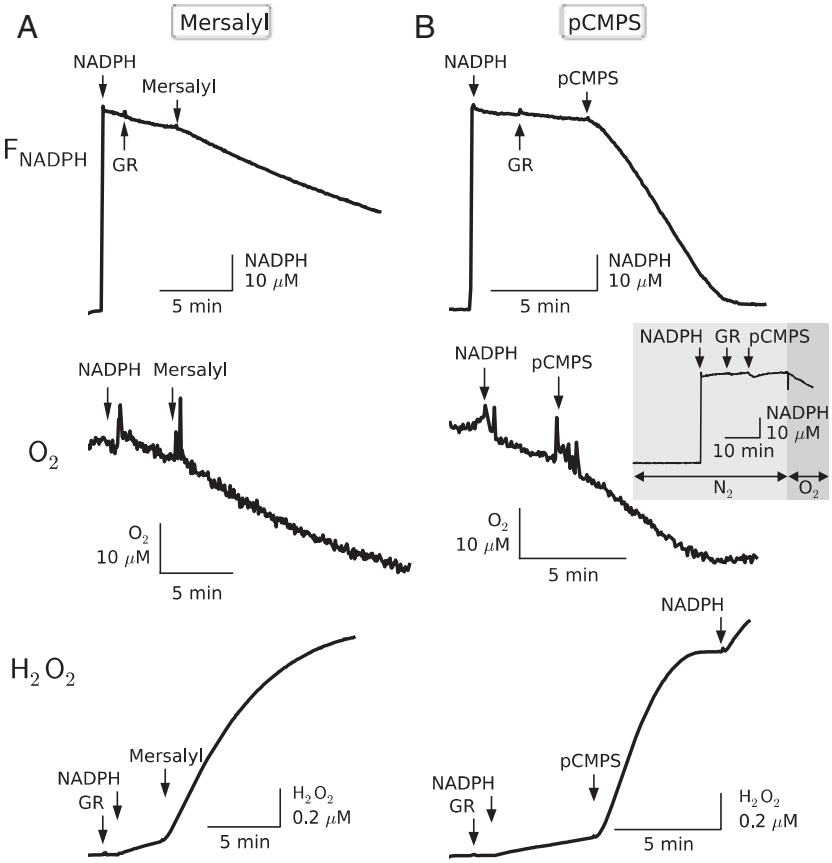

Fig. 3. NADPH consumption, O_2 consumption and H_2O_2 production rates by GR. A. Recombinant GR (200 nM) was added to KCl buffer in the absence of GSSG. Upon addition of NADPH, NADPH fluorescence (F_{NADPH}, upper trace), O_2 (middle trace) and H_2O_2 fluorescence (F_{H2O2}, lower trace) were recorded, before and after adding mersalyl (5 μM). B. Same, but with pCMPS (5 μM) in place of mersalyl. *Shaded inset* shows that during anoxia (N_2, lighter gray shaded area), GR (200 nM) and pCMPS (5 μM) did not induce any decrease in NADPH fluorescence until O_2 was readmitted (darker gray shaded area).

enhance NADPH-induced H_2O_2 production by TrxR1, Prx also prevented further increases in resorufin fluorescence (Fig. 5A, red and blue traces), indicating that continued H_2O_2 production by TrxR1 was masked by reduced Prx competing with HRP for H_2O_2. The masking effect of Prx on H_2O_2 production could be revealed by adding redox inert Zn^{2+} (blue trace), which is known to bind to accessible thiol groups [25]. Neither $ZnCl_2$ (20 μM), CDNB (50 μM) nor pCMPS (5 μM) had no significant effect on the Amplex UltraRed/HRP (resorufin) response to H_2O_2 in the buffer (Fig. 5B). Because Zn^{2+} had no significant effect on the ability of TrxR1 to generate H_2O_2 in the presence of NADPH and CDNB, Zn^{2+}'s effect at unmasking H_2O_2 production could be attributed to Prx inhibition. Removing Zn^{2+} from functionally important thiol groups by adding EDTA prevented further H_2O_2 spillover (Fig. 5A).

To mimic conditions in the mitochondrial matrix in which NADPH is generated endogenously from $NADP^+$ by matrix enzymes such as isocitrate dehydrogenase, we also incubated recombinant TrxR with purified isocitrate dehydrogenase, together with isocitrate and $NADP^+$ in KCl buffer containing EDTA to chelate free Mg^{2+} (Fig. 6A). When excess Mg^{2+} was added to activate NADPH generation by isocitrate dehydrogenase, H_2O_2 production increased gradually as NAPDH increased. Addition of the TrxR1 inhibitor CDNB (50 μM) significantly increased H_2O_2 production, similar to the effects of thiol reactive agents on NADPH-induced H_2O_2 production by GR (Fig. 2). In contrast, in the absence of TrxR1, isocitrate dehydrogenase activation by Mg^{2+} generated NADPH (Fig. 6B, top trace) but no significant H_2O_2 (bottom trace). Note that in these experiments we used a relatively high CDNB concentration (50–100 μM), because 100 μM is required for complete inhibition of isolated TrxR1 [26], although lower concentrations are able to induce H_2O_2 production to a lesser extent.

3.3. NADPH-dependent ROS production in isolated mitochondria

To determine whether NADPH-dependent ROS production by GR and TrxR2 occurs in isolated cardiac mitochondria subjected to reductive stress, we studied alamethicin-permeabilized mitochondria in which free (unbound) low molecular weight compounds like NADH/NAD^+, NADPH/$NADP^+$, GSH/GSSG, substrates, etc., equilibrate through alamethicin-induced membrane pores, while proteins and protein-bound metabolites are retained in the matrix [16]. In Fig. 7, mitochondria in sucrose buffer were permeabilized with alamethicine and then left unperturbed to allow endogenous GSH/GSSG and other small molecules to diffuse out of the matrix. After 5 min, addition of NADPH resulted in a marked increase in H_2O_2 production (red trace *a*). In contrast, addition of NADPH immediately after permeabilization had no effect on H_2O_2 production initially (blue trace *b*). The lack of H_2O_2 production immediately after permeabilization is likely due to an oxidized matrix environment characterized by high GSSG levels and low GSH [27]. Under these conditions, NADPH is consumed by GR for GSSG reduction rather than H_2O_2 production, until either the GSSG has all been converted to GSH and/or has diffused out of the matrix through alamethicine pores. After 5 min, however, addition of a second bolus of NADPH increased ROS production comparably to that in trace *a*.

It could be argued that when the GSH/GSSG pool was depleted by permeabilizing mitochondria in Fig. 7, the robust H_2O_2 production

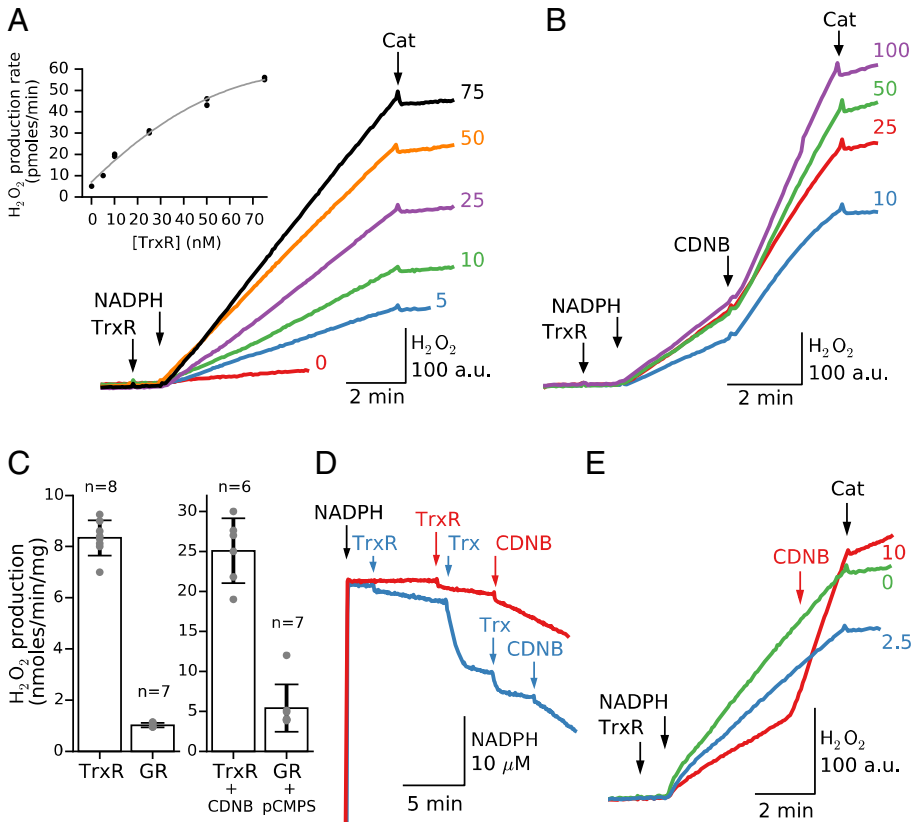

Fig. 4. Recombinant TrxR1 generates ROS when provided with exogenous NADPH. A. Rat recombinant TrxR1 was added to KCl buffer in the concentrations indicated (5–75 nM) at the end of traces. NADPH addition (100 μM) resulted in H_2O_2 production that was dependent on [TrxR1]. In the absence of TrxR1, the NADPH-induced non-specific increase in resorufin fluorescence was minimal (red trace 0). Inset to Fig. 4A shows H_2O_2 production in pmol/min for different TrxR1 concentrations ($n = 2$). B. H_2O_2 production by 50 nM TrxR1 was activated by NADPH added at the indicated concentrations (10, 25, 50 and 100 μM). Addition of 50 μM CDNB significantly accelerated ROS production at all NAPDH concentrations. C. Average H_2O_2 production by TrxR1 or GR expressed per mg of protein in the absence or presence of inhibitors (50 μM CDNB, 5 μM pCMPS). D. NADPH (50 μM) fluorescence in KCL buffer was stable until TrxR1 (50 nM) was added, initiating NADPH oxidation that was further accelerated by CDNB (50 μM) (red trace). Addition of oxidized Trx (10 followed by 2.5 μM) rapidly increased NADPH oxidation, which returned to the former rate after Trx was reduced. CDNB addition accelerated NADPH oxidation (red and blue trace). E. H_2O_2 production by 50 nM TrxR1 was initiated by 25 μM NADPH in the absence of Trx (green trace) or presence of 2.5 (blue trace) or 10 μM (red trace) oxidized Trx. Addition of 50 μM CDNB significantly accelerated depressed H_2O_2 production in the presence of Trx (red trace). (Additions to both traces are indicated by black arrows; additions to one trace only are indicated by the same color arrows).

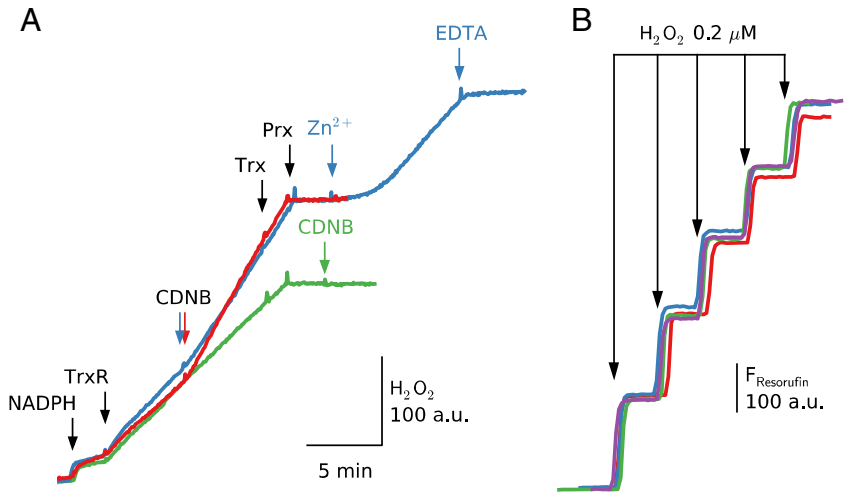

Fig. 5. Prx inhibition by Zn^{2+} unmasks NADPH-induced H_2O_2 production by TrxR1. A. NADPH (50 μM) and TrxR1 (50 nM) addition to KCl buffer initiated H_2O_2 production that was not significantly affected by 1 μM Trx, but was rapidly inhibited by adding Prx (100 nM), even after CDNB (50 μM) (green trace). Prx addition also stopped NADPH-induced H_2O_2 production by TrxR1 enhanced by CDNB (30 μM) (red and blue traces). Addition of $ZnCl_2$ (20 μM) to prevent Prx from reducing H_2O_2 partially reactivated H_2O_2 production and was reversed by adding EDTA (250 μM) to chelate Zn^{2+} (blue trace). Similar results were obtained in 4 preparations. (Additions to both traces are indicated by black arrows; additions to one trace only are indicated by the same color arrows). B. CDNB (50 μM, green trace), $ZnCl_2$ (20 μM, lilac trace) or pCMPS (5 μM, red trace), present in the buffer from the start, had no significant effect on Amplex UltraRed/HRP response to H_2O_2 additions (control, blue trace).

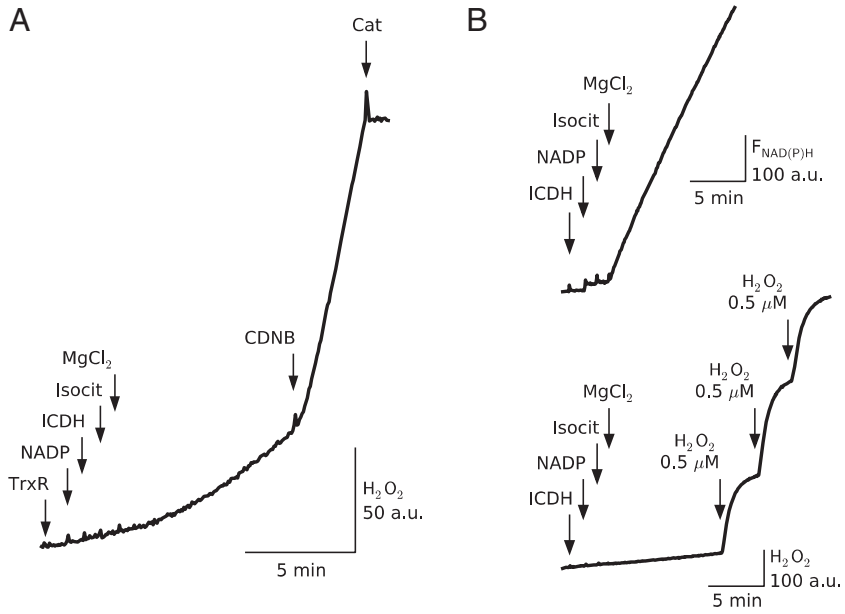

Fig. 6. A. Rat recombinant TrxR1 (50 nM) was incubated in KCl buffer containing 1 mM EDTA, 0.25 mM $NADP^+$, isocitrate dehydrogenase (ICDH) (3.6 μg protein) and 2 mM isocitrate (isocit). NADPH generation by ICDH was initiated by addition of 5 mM $MgCl_2$, causing a slowly accelerating increase in H_2O_2 production which was further significantly increased by 50 μM CDNB. B. In contrast, in the absence of TrxR, ICDH activation by Mg^{2+} generated NADPH (upper trace) but no significant H_2O_2 production (lower trace).

induced by NADPH was due to the loss of antioxidant power, rather than direct stimulation of ROS generation by GR and TR2. In this case, an alternative mechanism for NADPH-induced ROS generation would be required. NADH-related ROS production by electron chain complexes or NAD-related dehydrogenases is unlikely, because no exogenous substrates or NADH was provided after permeabilization, and most of the endogenous substrates and pyridine nucleotides would be expected to diffuse out of the matrix following membrane permeabilization, although some fraction may remain bound [28]. Even then, this fraction is likely to be oxidized in the absence of substrates [27]. This was confirmed in Fig. 8A (red trace a), which shows that addition of rotenone to inhibit complex I in permeabilized mitochondria did not result in significant H_2O_2 production, unless NADH was also added. Antimycin to inhibit complex III did not further potentiate H_2O_2 production under these conditions. NADH added before or after CDNB also did not result in significant H_2O_2 production, indicating that CDNB does not inhibit respiratory complexes to the extent required for ROS production (blue trace *b*). NADPH was specifically required to initiate H_2O_2 production by CDNB (green trace *c*). Note that the rate of NADPH-induced H_2O_2 production in the presence of CDNB in trace *c* was comparable to that of NADH-dependent H_2O_2 production when respiratory complexes were maximally inhibited by rotenone and antimycin in trace *a*, with rates averaging 0.35 nmoles/min/mg, 95% CI [0.34, 0.38], and 0.33 nmoles/min/mg, 95% CI [0.31, 0.38], respectively, in 4 paired mitochondria preparations (Fig. 8A, inset). Fig. 8B provides further evidence that CDNB did not inhibit respiratory chain activity in permeabilized mitochondria, since the rate of NADH oxidation was similar before or after CDNB was added (red trace *a*). In contrast, rotenone completely inhibited NADH oxidation (blue trace *b*). Similar findings were obtained using the TrxR inhibitor auranofin in place of CDNB (Fig. 8C & D). These findings were confirmed in 4 preparations, and together show that neither CDNB nor auranofin causes NADH-related ROS production by directly inhibiting respiratory complexes or stimulating ROS production by NADH-related TCA cycle dehydrogenases.

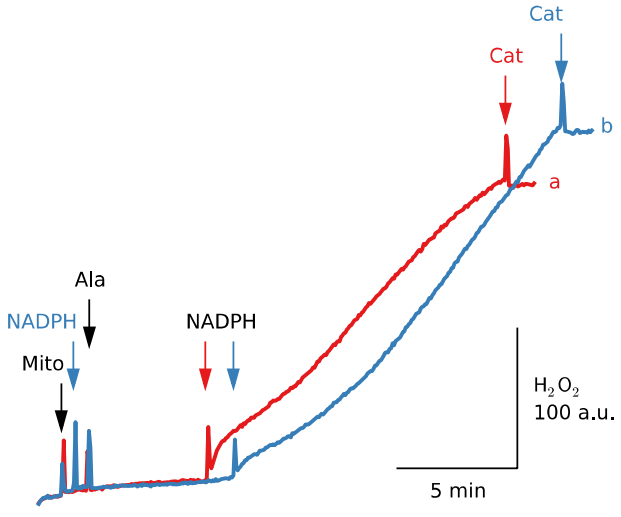

Fig. 7. NADPH-dependent H_2O_2 generation in permeabilized cardiac mitochondria. Mitochondria in sucrose buffer were permeabilized with alamethicine (ala). After waiting 5 min for endogenous GSH/GSSG and other small molecules to diffuse out of the matrix, 50 μM NADPH was added resulting in a marked increase in H_2O_2 production (red trace *a*). In contrast, addition of NADPH immediately after permeabilization had no effect on H_2O_2 production (blue trace *b*), but after 5 min, addition of a second 50 μM bolus of NADPH increased ROS production comparably to that in trace *a*. (Additions to both traces are indicated by black arrows; additions to one trace only are indicated by the same color arrows).

There are some reports that Nox4, a constitutively active NAPDH oxidase, may be present in the mitochondrial inner membrane, and could be a source of NADPH-dependent ROS production. To test this possibility, we obtained Nox4 −/− mice [29], a generous gift of Dr. Junichi Sadoshima, from which we isolated cardiac mitochondria. In response to CDNB or auranofin, H_2O_2 efflux from Nox4 −/− cardiac mitochondria was similar compared to wild-type murine cardiac mitochondria (Fig. 9), indicating the NADPH-induced ROS production under these conditions could not be attributed to Nox4 activity. In addition, incubation of permeabilized mitochondria from rabbit heart with 5 μM gr91ds-tat, considered to be a specific inhibitor of Nox2 [30], did not suppress NADPH-dependent H_2O_2 production induced by CDNB (results not shown).

These findings indicate that during reductive stress in permeabilized cardiac mitochondria, GR and/or TrxR2 can generate ROS spillover directly, at a rate comparable to NADH-related ROS production by inhibited respiratory chain complexes and/or NAD-related dehydrogenases. The

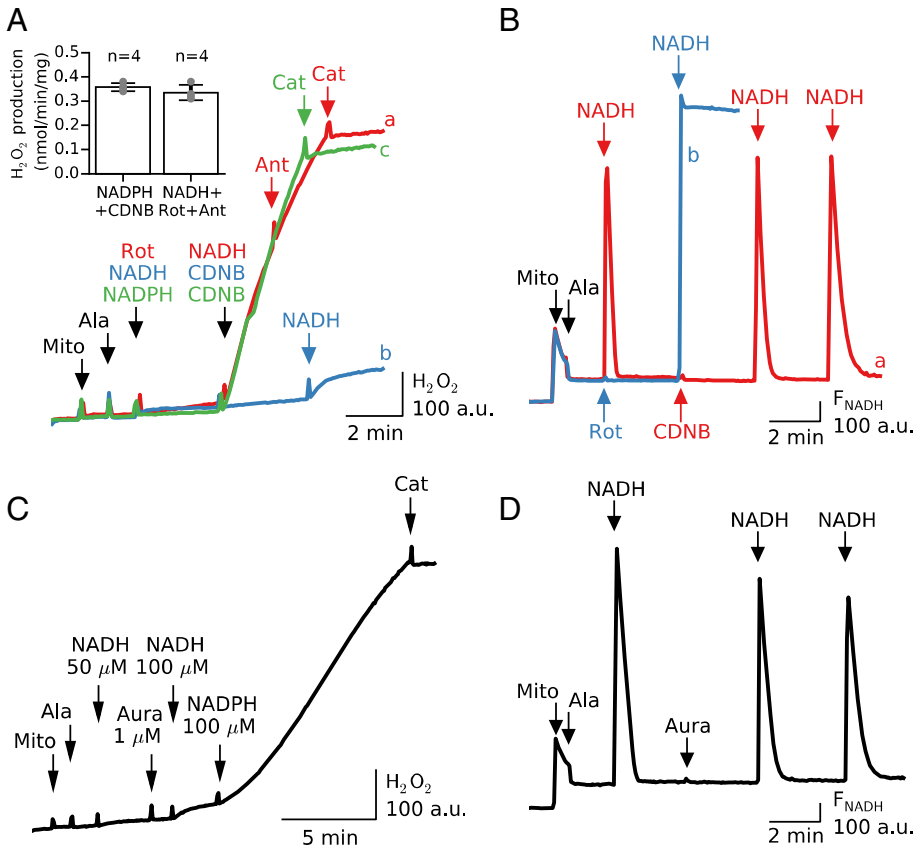

Fig. 8. Unlike NADPH, NADH does not increase H_2O_2 production in permeabilized mitochondria, either before or after adding CDNB or auranofin. A. After permeabilization with alamethicine (ala), mitochondria in sucrose buffer were exposed to either: 10 μM rotenone followed by 50 μM NADH followed by 5 μM antimycin (red trace *a*); 50 μM NADH followed by 100 μM CDNB followed by additional NADH (blue trace *b*); or 50 μM NADPH followed by 100 μM CDNB (green trace *c*). The rate of H_2O_2 production was quantitatively similar for NADPH + CDNB as for rotenone + NADH + antimycin (inset), but markedly less for NADH + CDNB. B. Mitochondria in sucrose buffer were permeabilized with alamethicine (ala). NADH (50 μM) was oxidized at a high rate before or after 100 μM CDNB was added (red trace *a*). In contrast, 10 μM rotenone completely prevented NADH oxidation (blue trace *b*). C. Mitochondria in sucrose buffer were permeabilized with alamethicine (ala). NADH added before or after 1 μM auranofin failed to generate significant H_2O_2, which required addition of NADPH. D. Mitochondria in sucrose buffer were permeabilized with alamethicine (ala). NADH (50 μM) was rapidly oxidized at a similar rate before or after 1 μM auranofin was added. (Additions to both traces are indicated by black arrows; additions to one trace only are indicated by the same color arrows).

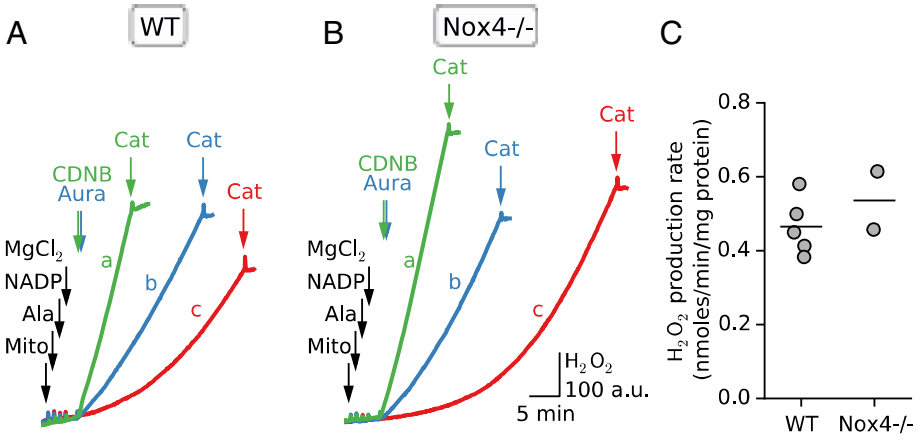

Fig. 9. CDNB- and auranofin-induced H_2O_2 production is similar in alamethicin-permeabilized cardiac mitochondria isolated from wild-type and Nox4 −/− mice. A. Cardiac mitochondria isolated from wild-type mice incubated in EDTA-sucrose buffer were permeabilized with alamethicin (ala). $NADP^+$ (0.5 μM), malate and isocitrate (2.5 mM each) were added, after which NADPH production was initiated by activating malate- and isocitrate dehydrogenase with excess Mg^{2+}. H_2O_2 production rapidly increased when CDNB (50 μM, trace *a*) or auranofin (1 μM, trace *b*) was added, compared to control conditions without inhibitors (trace *c*). Note that additions to all superimposed traces are indicated by black type, whereas additions specific to each colored trace are indicated by the same color type. B. Same protocol with cardiac mitochondria isolated from Nox4 −/− mice, showing similar levels of H_2O_2 production as wild-type mice in A. (Additions to both traces are indicated by black arrows; additions to one trace only are indicated by the same color arrows). C. Comparison of the maximum rates of H_2O_2 production (nmol/min/mg protein) in wild-type versus Nox4 −/− mice.

quantitative contributions of GR versus TrxR2 to total ROS production in permeabilized mitochondria, however, are difficult to assess. Even with GSSG/GSH depleted by permeabilization, Prx remained effective at masking H_2O_2 production. This is demonstrated in Fig. 10A, in which alamethicin-treated mitochondria were incubated with CDNB in the absence (blue trace) or presence of Zn^{2+} at concentrations of 5 (red trace), 10 (green trace) or 20 (dashed line) μM. Zn^{2+} significantly enhanced NADPH-induced H_2O_2 production, which saturated at 10 μM (Fig. 10B).

4. Discussion

4.1. Major findings of this study

Our major novel finding is the demonstration that both reduced GR and TrxR's, like other members of the disulfide reductase flavoenzyme family including lipoamide dehydrogenase (the E3 component of alpha-ketoglutarate dehydrogenase and pyruvate dehydrogenase), can leak electrons to O_2 and generate significant amounts of ROS spillover when the supply of their natural electron acceptors is limited or electron transport to acceptors is inhibited (Fig. 1). Similar to these enzymes, reduced flavoprotein in isolated complex I has also been directly demonstrated to generate significant ROS [31] in the absence of electron acceptors other than O_2 or when intrinsic electron transport to electron acceptors is prevented by inhibitors. Therefore, thermodynamically, in the absence of electron transport or acceptors, ROS production by all these proteins is defined by NAD(P)H/NAD(P)$^+$ ratio and hence by the fraction of flavin in a fully reduced state. Whether endogenous mechanisms in intact cells, however, are able to induce redox modifications that inhibit intrinsic electron transport to target substrates and generate sufficiently reduced flavin to account for the ROS generation observed during reductive stress, however, still remains to be directly demonstrated. Nevertheless, our findings indicate that GR and TrxR2 need to be factored into this equation.

Using the Amplex UltraRed/HRP system to detect H_2O_2 from resorufin fluorescence, we have shown that both GR and TrxR's produce H_2O_2 in the presence of NADPH and O_2. Reduced flavoproteins are known to be oxidized by molecular O_2 with formation of $O_2^{\bullet-}$ and H_2O_2 [32], and H_2O_2 formation by lipoamine dehydrogenase [33] and Nox4 [34] has been directly demonstrated. The lack of an effect of SOD on H_2O_2 production by these proteins suggests that spontaneous dismutation of $O_2^{\bullet-}$ to H_2O_2 is not rate-limiting [35]. Acceleration of non-enzymatic dismutation has been shown with Nox4 [34], and may be the reason why many oxidases (glucose, xanthine oxidase) are known to produce mainly H_2O_2. Whereas lipoamide dehydrogenase uses NADH as its preferred electron donor, GR and TrxR's use NADPH exclusively for this purpose. These results provide new insights into how reductive stress generates net ROS production, by converting enzymes that normally serve antioxidant functions into ROS producers.

The link between reductive stress and oxidative injury has been substantiated at multiple levels, including the *in vivo* setting. For example, mutations in α_B-crystallin, a small heat shock protein, result in protein aggregation causing cardiomyopathy in mice. The mechanism underlying protein aggregation disease has been attributed to reductive stress associated with increased activity of glucose-6-phosphate dehydrogenase (G6PD) raising NADPH levels [10]. In studies of experimental heart failure, G6PD activity was found to be significantly elevated resulting in a two-fold increase in NADPH concentration and increased ROS production [9]. In cultured cells, reductive stress associated with increased GSH levels has shown to trigger mitochondrial oxidation and cytotoxicity, although no increase in ROS production was reported based on DCF fluorescence [7]. Long-term treatment of mice with dioxin resulted in increased GSH levels in liver mitochondria that significantly enhanced $O_2^{\bullet-}$ and H_2O_2 production by mitochondria [8]. These findings are consistent with the "redox-optimized ROS balance" hypothesis put forward by O'Rourke's group [11,12], which posits that redox balance is lost and ROS production increases at both extremes of oxidation and reduction of redox couples involved in respiratory chain activity (NADH/NAD$^+$) or ROS scavenging (NADPH/NADP$^+$, GSH/GSSG). In addition, their recent work [12] shows that mitochondrial bioenergetics and ROS production are closely linked, such that reductive stress may also compromise cellular function by impairing energy production as well as by promoting oxidative injury.

Our findings provide novel insights into the "redox-optimized ROS balance" hypothesis showing that the previous assumption that NAD$^+$-related ROS production from respiratory complexes and/or NADH-related dehydrogenases simply overwhelms the capacity of NADPH-dependent ROS scavenging during reductive stress is not the full story. The novel information provided here is that ROS-scavenging capacity by both the glutathione/Gpx/GR and Prx/Trx/TrxR2 systems

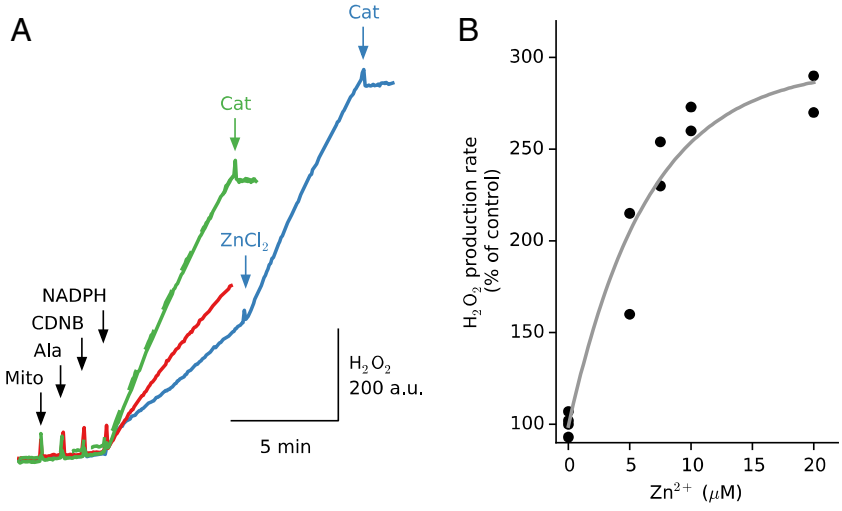

Fig. 10. Effect of Prx inhibition by Zn^{2+} on CDNB-induced H_2O_2 production in permeabilized mitochondria. A. Mitochondria were incubated in the absence (blue trace) or presence of 5 μM (red trace), 10 μM (green trace) or 20 μM (green dashed line) Zn^{2+}. After permeabilization with alamethicine (Ala) and addition of CDNB (30 μM), NADPH (50 μM) was added to initiate H_2O_2 production. In the presence of Zn^{2+}, H_2O_2 production was significantly enhanced (red and green traces), saturating at 10 μM. In the blue trace, 20 μM of Zn^{2+} was added after 8 min, and also accelerated H_2O_2 production. (Additions to both traces are indicated by black arrows; additions to one trace only are indicated by the same color arrows). B. Zn^{2+}-stimulated increase in ROS production, relative the rate of H_2O_2 production with no Zn^{2+} (100%), in 2 preparations.

may become severely impaired during reductive stress due to the conversion of GR and TrxR2 into ROS producers, as a result of NADPH-dependent electron leak to O_2 when their usual electron acceptors are in limited supply.

The evidence can be summarized as follows: 1) purified recombinant GR and TrxR1 both generated substantial amounts of H_2O_2 when supplied with NADPH in the absence of their usual electron acceptors GSSG and oxidized Trx, or if electron flow to their natural electron acceptors was impaired by thiol reactive agents such as pCMPS, mersalyl or pCMB for GR and CDNB for TrxR2 (Figs. 2 & 4); 2) in permeabilized mitochondria in which no NADH was provided for ROS generation by respiratory complexes or NAD^+-related matrix dehydrogenases, NADPH stimulated robust H_2O_2 production when GR and TrxR2 were inhibited by lack of GSSG and/or CDNB (Fig. 8). Under these conditions, addition of NADH did not induce H_2O_2 production, indicating that these thiol reactive agents did not inhibit respiratory chain complexes directly at the concentrations used (Fig. 8); 3) in permeabilized mitochondria, the rate of NADPH-dependent H_2O_2 production by inhibited GR and TrxR2 during reductive stress was quantitatively comparable to the rate of NADH-dependent H_2O_2 production when respiratory complexes were maximally inhibited by rotenone and antimycin; 4) we also excluded the possibility that endogenous matrix Nox4 or Nox2 are responsible for NADPH-dependent ROS generation (Fig. 9). However, these observations notwithstanding, it still remains to be proved whether conditions sufficient to activate ROS production by GR and TrxR2 occur in intact mitochondria during reductive stress *in vivo*. Although not applicable to permeabilized mitochondria, it should be mentioned that in intact mitochondria transhydrogenase is a major mechanism responsible for the transfer of reducing equivalents between NAD(H) and NADP(H), coupled to the translocation of protons across inner membrane. Under physiological conditions about half of NADPH production is abolished by uncouplers, consistent with transhydrogenase-generated NADPH, with similar estimates from flux measurements [36].

4.2. Mechanisms of ROS generation by GR and TrxR's

Although ROS production by GR has not, to our knowledge, been previously reported, TrxR1 was reported to be irreversibly inhibited by CDNB resulting in NADPH oxidation in the presence of NADPH and O_2 almost 20 years ago [26]. Later studies showed that one of the ROS species generated by CDNB-inhibited TrxR1 was superoxide, since $O_2^{\bullet-}$ detection (by the adrenochrome method) was eliminated by SOD [37]. In the absence of thioredoxin, $O_2^{\bullet-}$ production by TrxR1 was also demonstrated using the EPR spin trap DEPMPO method [14]. However, as we have shown above in the presence of NADPH, TrxR1 also generates H_2O_2 (Fig. 4) that is likely due to accelerated spontaneous dismutation of $O_2^{\bullet-}$ as described above. TrxR1's proposed inherent NADPH oxidase activity [14] can also be induced by inhibiting electron flow to Trx with low molecular weight compounds like auranofin, curcumin, juglone, motexan gadolinium and other dinitrohalobenzenes [14,37–40], resulting in ROS production. As shown in Fig. 3, the rate of NADPH oxidation by GR was fully accounted for by the rate of O_2 consumption, but both NADPH and O_2 consumption were considerably greater than the rate of H_2O_2 production. The quantitative analysis indicated that only about 15% the electron leak from GR produces H_2O_2 directly by two-electron reduction. An important point to note is that the maximal rate of electron leak by GR to form H_2O_2 and reduce other possible ROS is orders of magnitude lower than its capacity to transfer electrons to GSSG. This is obvious in Fig. 2D, in which the rate of NADPH consumption associated with H_2O_2 production by GR in the absence of GSSG is orders of magnitude slower than when GSSG is added to the cuvette. Thus, O_2 becomes viable as an electron acceptor from the flavoprotein redox site of GR only when the rate of electron transfer to GSSG is markedly impaired. Nevertheless, this low level of NADPH oxidase activity is still sufficient to generate significant amounts of H_2O_2, at rates comparable to the inhibited respiratory chain complexes during reductive stress (Fig. 8A).

4.3. Physiological implications, limitations and significance

To protect matrix elements against oxidative damage by ROS, mitochondria have evolved an integrated set of thiol systems. The glutathione/Gpx1/GR and Prx/Trx/TrxR2 systems are most important, although catalase is also present in the matrix [4,5] and may come into play at micromolar concentrations of H_2O_2 [6]. Under normal conditions, H_2O_2 efflux from mitochondria energized with NAD^+-related substrates is very low, suggesting that NADPH-dependent H_2O_2 scavenging is able to balance H_2O_2 production in the matrix. At either extreme of redox balance, however, this is no longer the case. This is obvious for oxidative stress, which is defined by excess ROS production relative to ROS scavenging. For reductive stress, however, the cause of the imbalance is less obvious, since both NADH-dependent ROS production and NADPH-dependent ROS scavenging normally increase in parallel. The finding that NADPH-dependent ROS scavenging is directly impaired by the conversion of GR and TrxR2 from their antioxidant functions into ROS producers during reductive stress offers a resolution to this seeming paradox.

In addition to direct ROS production by GR and TrxR2, however, we also found that Prx activity has important influences on the degree of ROS spillover from the matrix during reductive stress. Specifically, we found that although there is an oxidized Trx concentration-dependent depression of H_2O_2 production (Fig. 4E) by TrxR's, for normal NADPH and Trx concentrations inside the matrix (about 200 μM and <10 μM correspondingly), Trx will be rapidly reduced (Fig. 4D) allowing H_2O_2 production to continue. However, the expected increase in $[H_2O_2]$ was partly masked by Prx rapidly reducing the generated H_2O_2, as demonstrated when Zn^{2+} was used to inhibit Prx in Figs. 5A and 10. Therefore, it seems that H_2O_2 production by TrxR2/NADPH is not the primary determinant of matrix H_2O_2 spillover, but rather Prx activity. This could be an important regulatory mechanism for redox signaling or other purposes. Although free Zn^{2+} concentration is normally very low, metallothionein, the main Zn^{2+} binding protein in the cytoplasm, releases Zn^{2+} from its thiols. Metallothionein thiols have very low redox potential and are readily oxidized to release Zn^{2+} [41] even by relatively mild oxidants. This initial cytoplasmic Zn^{2+} release, if induced by ROS production from respiratory chain complexes or matrix dehydrogenases, can be can taken up into the matrix by the Ca^{2+}-uniporter as well as through independent import mechanism that is still not well defined [41]. In addition mitochondria have been shown to contain an independent store of Zn^{2+} that can be mobilized [42]. Zn^{2+} has been repeatedly shown to increase mitochondrial ROS production [41]. Although Prx is thought to be responsible for scavenging most of the H_2O_2 produced in the matrix [43], this could be an overestimate [23] and the relative contribution of other antioxidant systems requires further clarification. In this regard, one problem is that chemicals used to "selectively and independently" inhibit GSH/Trx systems are not completely specific: GSH depletion with CDNB, which is a good substrate for glutathione-S-transferase, also inhibits TrxR activity with a concomitant increase in ROS production. Significant inhibition of TrxR activity (>50%) has been reported at low concentrations of CDNB (≤10 μM) and this effect was almost 10,000-fold faster than alkylation of GSH [26]. Irrespective of these issues, Prx inhibition by Zn^{2+} could be an important step that increases matrix H_2O_2 levels, further exacerbating ROS spillover during reductive stress. Ischemia/reperfusion, ROS and peroxynitrite have been shown to cause significant cytoplasmic and mitochondrial Zn^{2+} release in cardiomyocytes as demonstrated by high-affinity Zn^{2+} selective probes [44]. In addition, exogenous Zn^{2+} delivered either at the onset of reoxygenation/reperfusion (mimicking post-conditioning) or before ischemia (mimicking pre-conditioning) is cardioprotective [45–49], attributed to Zn^{2+}-induced activation of the RISK pathway inhibiting mitochondrial permeability transition pore opening upon reperfusion [45,50,51]. Since cardioprotection by pre- and post-conditioning ischemia can be abolished by ROS

scavengers [52], our findings raise the intriguing possibility that Zn^{2+} release may contribute to RISK pathway activation by inhibiting Prx activity and promoting ROS spillover. On the other hand, after prolonged ischemia/reperfusion, Zn^{2+} release causing Prx inhibition could be a factor exacerbating the massive ROS burst upon reperfusion that has cytotoxic effects. Further experiments will be required to delineate the regulation of Zn^{2+} release by endogenous and exogenous factors as a cardioprotective versus injurious factor in the setting of ischemia/reperfusion.

An important limitation of our study is that our findings were all obtained using purified recombinant enzymes or isolated permeabilized mitochondria. We cannot exclude the possibility that GR and TrxR2 might behave differently in intact mitochondria *in vivo*, even though the relationship between reductive stress and oxidative injury *in vivo* is well-established, as reviewed above. Also, due to the lack of availability of recombinant TrxR2 with intact activity, we used recombinant TrxR1 as a proxy assuming that its properties are similar. In permeabilized mitochondria with both GR and TrxR2 present, we could not quantitatively assess their separate contributions to total H_2O_2 spillover. However, assuming that TrxR2 behaves similarly to recombinant TrxR1, then it is likely to make an important contribution for two reasons: 1) the capacity of recombinant TrxR1 to generate NADPH-dependent H_2O_2 was 8-fold higher than recombinant GR (Fig. 4C); and 2) in the matrix GSH/GSSG levels are present at millimolar levels, whereas Trx is present at micromolar levels [23], suggesting that depletion of oxidized Trx may occur more readily than depletion of GSSG. Finally, although our experiments in Fig. 8 show that the combined capacity of GR and TrxR2 to generate H_2O_2 is quantitatively comparable to the respiratory chain under artificially maximized conditions of reductive stress, whether this accurately reflects the relative contributions of these processes during reductive stress under physiological conditions in intact cells or tissue is difficult to assess. It is also possible that other NADPH-dependent reductases, such as isocitrate dehydrogenase, malic enzyme or glutamate dehydrogenase, can generate ROS when their natural electron acceptors are in limited availability. Further studies will be required to address these important issues which impact oxidative tissue injury during reductive stress. Targeting these enzymes, especially the Prx/Trx/TrxR2 pathway, to promote cardioprotective signaling pathway activation and reduce ischemia/reperfusion damage in heart, or to increase oxidative injury when desirable, such as in cancer treatment, may have therapeutic promise. Indeed, TrxR inhibitors have been explored as anti-cancer compounds [38,40,53–56], and our findings suggest that GR inhibitors may have similar, and possibly synergistic, potential.

Conflict of interest

None.

Acknowledgments

We thank Junichi Sadoshima, MD, PhD, for generously providing the Nox4 −/− mice for our studies. This work was supported by NIH/NHLBI grants R01 HL101228, R01 HL117385, AHA Western States Affiliate Post-doctoral Research Fellowship 11POST6110007, and the Laubisch and Kawata Endowments. GC was supported by a Postdoctoral Fellowship award (No. 11POST6110007) from the American Heart Association, Western States Affiliate.

References

[1] E.S. Christians, I.J. Benjamin, Proteostasis and REDOX state in the heart, Am. J. Physiol. Heart Circ. Physiol. 302 (2012) H24–H37.
[2] M.P. Murphy, How mitochondria produce reactive oxygen species, Biochem. J. 417 (2009) 1–13.
[3] A.V. Kareyeva, V.G. Grivennikova, A.D. Vinogradov, Mitochondrial hydrogen peroxide production as determined by the pyridine nucleotide pool and its redox state, Biochim. Biophys. Acta 1817 (2012) 1879–1885.
[4] M. Salvi, V. Battaglia, A.M. Brunati, N. La Rocca, E. Tibaldi, P. Pietrangeli, L. Marcocci, B. Mondovi, C.A. Rossi, A. Toninello, Catalase takes part in rat liver mitochondria oxidative stress defense, J. Biol. Chem. 282 (2007) 24407–24415.
[5] R. Radi, J.F. Turrens, L.Y. Chang, K.M. Bush, J.D. Crapo, B.A. Freeman, Detection of catalase in rat heart mitochondria, J. Biol. Chem. 266 (1991) 22028–22034.
[6] D.E. Heck, M. Shakarjian, H.D. Kim, J.D. Laskin, A.M. Vetrano, Mechanisms of oxidant generation by catalase, Ann. N. Y. Acad. Sci. 1203 (2010) 120–125.
[7] H. Zhang, P. Limphong, J. Pieper, Q. Liu, C.K. Rodesch, E. Christians, I.J. Benjamin, Glutathione-dependent reductive stress triggers mitochondrial oxidation and cytotoxicity, FASEB J. 26 (2012) 1442–1451.
[8] D. Shen, T.P. Dalton, D.W. Nebert, H.G. Shertzer, Glutathione redox state regulates mitochondrial reactive oxygen production, J. Biol. Chem. 280 (2005) 25305–25312.
[9] S.A. Gupte, R.J. Levine, R.S. Gupte, M.E. Young, V. Lionetti, V. Labinskyy, B.C. Floyd, C. Ojaimi, M. Bellomo, M.S. Wolin, F.A. Recchia, Glucose-6-phosphate dehydrogenase-derived NADPH fuels superoxide production in the failing heart, J. Mol. Cell. Cardiol. 41 (2006) 340–349.
[10] N.S. Rajasekaran, P. Connell, E.S. Christians, L.J. Yan, R.P. Taylor, A. Orosz, X.Q. Zhang, T.J. Stevenson, R.M. Peshock, J.A. Leopold, W.H. Barry, J. Loscalzo, S.J. Odelberg, I.J. Benjamin, Human alpha B-crystallin mutation causes oxido-reductive stress and protein aggregation cardiomyopathy in mice, Cell 130 (2007) 427–439.
[11] M.A. Aon, S. Cortassa, B. O'Rourke, Redox-optimized ROS balance: a unifying hypothesis, Biochim. Biophys. Acta 1797 (2010) 865–877.
[12] S. Cortassa, B. O'Rourke, M.A. Aon, Redox-optimized ROS balance and the relationship between mitochondrial respiration and ROS, Biochim. Biophys. Acta 1837 (2014) 287–295.
[13] C.L. Quinlan, R.L. Goncalves, M. Hey-Mogensen, N. Yadava, V.I. Bunik, M.D. Brand, The 2-oxoacid dehydrogenase complexes in mitochondria can produce superoxide/hydrogen peroxide at much higher rates than complex I, J. Biol. Chem. 289 (2014) 8312–8325.
[14] Q. Cheng, W.E. Antholine, J.M. Myers, B. Kalyanaraman, E.S. Arner, C.R. Myers, The selenium-independent inherent pro-oxidant NADPH oxidase activity of mammalian thioredoxin reductase and its selenium-dependent direct peroxidase activities, J. Biol. Chem. 285 (2010) 21708–21723.
[15] P. Korge, H.M. Honda, J.N. Weiss, Regulation of the mitochondrial permeability transition by matrix Ca(2+) and voltage during anoxia/reoxygenation, Am. J. Physiol. Cell Physiol. 280 (2001) C517–C526.
[16] I.S. Gostimskaya, V.G. Grivennikova, T.V. Zharova, L.E. Bakeeva, A.D. Vinogradov, In situ assay of the intramitochondrial enzymes: use of alamethicin for permeabilization of mitochondria, Anal. Biochem. 313 (2003) 46–52.
[17] P. Korge, P. Ping, J.N. Weiss, Reactive oxygen species production in energized cardiac mitochondria during hypoxia/reoxygenation: modulation by nitric oxide, Circ. Res. 103 (2008) 873–880.
[18] S. Nakagawa, I.C. Cuthill, Effect size, confidence interval and statistical significance: a practical guide for biologists, Biol. Rev. Camb. Philos. Soc. 82 (2007) 591–605.
[19] B. Efron, R. Tibshirani, Statistical data analysis in the computer age, Science 253 (1991) 390–395.
[20] G. Calmettes, G.B. Drummond, S.L. Vowler, Making do with what we have: use your bootstraps, J. Physiol. 590 (2012) 3403–3406.
[21] R.F. Colman, S. Black, On the role of flavin adenine dinucleotide and thiol groups in the catalytic mechanism of yeast glutathione reductase, J. Biol. Chem. 240 (1965) 1796–1803.
[22] L.D. Gorsky, D.R. Koop, M.J. Coon, On the stoichiometry of the oxidase and monooxygenase reactions catalyzed by liver microsomal cytochrome P-450. Products of oxygen reduction, J. Biol. Chem. 259 (1984) 6812–6817.
[23] B.A. Stanley, V. Sivakumaran, S. Shi, I. McDonald, D. Lloyd, W.H. Watson, M.A. Aon, N. Paolocci, Thioredoxin reductase-2 is essential for keeping low levels of H(2)O(2) emission from isolated heart mitochondria, J. Biol. Chem. 286 (2011) 33669–33677.
[24] C.C. Winterbourn, The biological chemistry of hydrogen peroxide, Methods Enzymol. 528 (2013) 3–25.
[25] N.J. Pace, E. Weerapana, Zinc-binding cysteines: diverse functions and structural motifs, Biomolecules 4 (2014) 419–434.
[26] E.S. Arner, M. Bjornstedt, A. Holmgren, 1-Chloro-2,4-dinitrobenzene is an irreversible inhibitor of human thioredoxin reductase. Loss of thioredoxin disulfide reductase activity is accompanied by a large increase in NADPH oxidase activity, J. Biol. Chem. 270 (1995) 3479–3482.
[27] J. Garcia, D. Han, H. Sancheti, L.P. Yap, N. Kaplowitz, E. Cadenas, Regulation of mitochondrial glutathione redox status and protein glutathionylation by respiratory substrates, J. Biol. Chem. 285 (2010) 39646–39654.
[28] K. Blinova, S. Carroll, S. Bose, A.V. Smirnov, J.J. Harvey, J.R. Knutson, R.S. Balaban, Distribution of mitochondrial NADH fluorescence lifetimes: steady-state kinetics of matrix NADH interactions, Biochemistry 44 (2005) 2585–2594.
[29] J. Kuroda, T. Ago, S. Matsushima, P. Zhai, M.D. Schneider, J. Sadoshima, NADPH oxidase 4 (Nox4) is a major source of oxidative stress in the failing heart, Proc. Natl. Acad. Sci. U. S. A. 107 (2010) 15565–15570.
[30] G. Csanyi, E. Cifuentes-Pagano, I. Al Ghouleh, D.J. Ranayhossaini, L. Egana, L.R. Lopes, H.M. Jackson, E.E. Kelley, P.J. Pagano, Nox2 B-loop peptide, Nox2ds, specifically inhibits the NADPH oxidase Nox2, Free Radic. Biol. Med. 51 (2011) 1116–1125.
[31] L. Kussmaul, J. Hirst, The mechanism of superoxide production by NADH:ubiquinone oxidoreductase (complex I) from bovine heart mitochondria, Proc. Natl. Acad. Sci. U. S. A. 103 (2006) 7607–7612.
[32] V. Massey, Activation of molecular oxygen by flavins and flavoproteins, J. Biol. Chem. 269 (1994) 22459–22462.
[33] L. Tretter, V. Adam-Vizi, Generation of reactive oxygen species in the reaction catalyzed by alpha-ketoglutarate dehydrogenase, J. Neurosci. 24 (2004) 7771–7778.

[34] I. Takac, K. Schroder, L. Zhang, B. Lardy, N. Anilkumar, J.D. Lambeth, A.M. Shah, F. Morel, R.P. Brandes, The E-loop is involved in hydrogen peroxide formation by the NADPH oxidase Nox4, J. Biol. Chem. 286 (2011) 13304–13313.
[35] K.R. Pryde, J. Hirst, Superoxide is produced by the reduced flavin in mitochondrial complex I: a single, unified mechanism that applies during both forward and reverse electron transfer, J. Biol. Chem. 286 (2011) 18056–18065.
[36] J. Rydstrom, Mitochondrial NADPH, transhydrogenase and disease, Biochim. Biophys. Acta 1757 (2006) 721–726.
[37] J. Nordberg, L. Zhong, A. Holmgren, E.S. Arner, Mammalian thioredoxin reductase is irreversibly inhibited by dinitrohalobenzenes by alkylation of both the redox active selenocysteine and its neighboring cysteine residue, J. Biol. Chem. 273 (1998) 10835–10842.
[38] J. Fang, J. Lu, A. Holmgren, Thioredoxin reductase is irreversibly modified by curcumin: a novel molecular mechanism for its anticancer activity, J. Biol. Chem. 280 (2005) 25284–25290.
[39] N. Cenas, H. Nivinskas, Z. Anusevicius, J. Sarlauskas, F. Lederer, E.S. Arner, Interactions of quinones with thioredoxin reductase: a challenge to the antioxidant role of the mammalian selenoprotein, J. Biol. Chem. 279 (2004) 2583–2592.
[40] S.I. Hashemy, J.S. Ungerstedt, F. Zahedi Avval, A. Holmgren, Motexafin gadolinium, a tumor-selective drug targeting thioredoxin reductase and ribonucleotide reductase, J. Biol. Chem. 281 (2006) 10691–10697.
[41] M.C. McCord, E. Aizenman, The role of intracellular zinc release in aging, oxidative stress, and Alzheimer's disease, Front. Aging Neurosci. 6 (2014) 77.
[42] S.L. Sensi, D. Ton-That, P.G. Sullivan, E.A. Jonas, K.R. Gee, L.K. Kaczmarek, J.H. Weiss, Modulation of mitochondrial function by endogenous Zn2+ pools, Proc. Natl. Acad. Sci. U. S. A. 100 (2003) 6157–6162.
[43] A.G. Cox, A.G. Pearson, J.M. Pullar, T.J. Jonsson, W.T. Lowther, C.C. Winterbourn, M.B. Hampton, Mitochondrial peroxiredoxin 3 is more resilient to hyperoxidation than cytoplasmic peroxiredoxins, Biochem. J. 421 (2009) 51–58.
[44] C.L. Lin, H.C. Tseng, R.F. Chen, W.P. Chen, M.J. Su, K.M. Fang, M.L. Wu, Intracellular zinc release-activated ERK-dependent GSK-3beta-p53 and Noxa-Mcl-1 signaling are both involved in cardiac ischemic–reperfusion injury, Cell Death Differ. 18 (2011) 1651–1663.
[45] G. Chanoit, S. Lee, J. Xi, M. Zhu, R.A. McIntosh, R.A. Mueller, E.A. Norfleet, Z. Xu, Exogenous zinc protects cardiac cells from reperfusion injury by targeting mitochondrial permeability transition pore through inactivation of glycogen synthase kinase-3beta, Am. J. Physiol. Heart Circ. Physiol. 295 (2008) H1227–H1233.
[46] G. Karagulova, Y. Yue, A. Moreyra, M. Boutjdir, I. Korichneva, Protective role of intracellular zinc in myocardial ischemia/reperfusion is associated with preservation of protein kinase C isoforms, J. Pharmacol. Exp. Ther. 321 (2007) 517–525.
[47] R. McIntosh, S. Lee, A.J. Ghio, J. Xi, M. Zhu, X. Shen, G. Chanoit, D.A. Zvara, Z. Xu, The critical role of intracellular zinc in adenosine A(2) receptor activation induced cardioprotection against reperfusion injury, J. Mol. Cell. Cardiol. 49 (2010) 41–47.
[48] K. Viswanath, S. Bodiga, V. Balogun, A. Zhang, V.L. Bodiga, Cardioprotective effect of zinc requires ErbB2 and Akt during hypoxia/reoxygenation, Biometals 24 (2011) 171–180.
[49] S.R. Powell, D. Hall, L. Aiuto, R.A. Wapnir, S. Teichberg, A.J. Tortolani, Zinc improves postischemic recovery of isolated rat hearts through inhibition of oxidative stress, Am. J. Physiol. 266 (1994) H2497–H2507.
[50] S. Lee, G. Chanoit, R. McIntosh, D.A. Zvara, Z. Xu, Molecular mechanism underlying Akt activation in zinc-induced cardioprotection, Am. J. Physiol. Heart Circ. Physiol. 297 (2009) H569–H575.
[51] M.M. Mocanu, D.M. Yellon, Letter to the editor: "Zinc and cardioprotection: the missing link", Am. J. Physiol. Heart Circ. Physiol. 296 (2009) H233–H234 (author reply H235).
[52] C. Penna, D. Mancardi, R. Rastaldo, P. Pagliaro, Cardioprotection: a radical view Free radicals in pre and postconditioning, Biochim. Biophys. Acta 1787 (2009) 781–793.
[53] J.E. Biaglow, R.A. Miller, The thioredoxin reductase/thioredoxin system: novel redox targets for cancer therapy, Cancer Biol. Ther. 4 (2005) 6–13.
[54] S. Li, J. Zhang, J. Li, D. Chen, M. Matteucci, J. Curd, J.X. Duan, Inhibition of both thioredoxin reductase and glutathione reductase may contribute to the anticancer mechanism of TH-302, Biol. Trace Elem. Res. 136 (2010) 294–301.
[55] K.F. Tonissen, G. Di Trapani, Thioredoxin system inhibitors as mediators of apoptosis for cancer therapy, Mol. Nutr. Food Res. 53 (2009) 87–103.
[56] Y. Liu, Y. Li, S. Yu, G. Zhao, Recent advances in the development of thioredoxin reductase inhibitors as anticancer agents, Curr. Drug Targets 13 (2012) 1432–1444.